The 2010 IEEE/RSJ International Conference on
Intelligent Robots and Systems
October 18-22, 2010, Taipei, Taiwan

# Adaptive Control for the Synchronization of Multiple Robot Manipulators with Coupling Time-Delays

Emmanuel Nuño[1,2], Luis Basañez[2] and Romeo Ortega[3]

***Abstract*— Two controllers capable of achieving asymptotic convergence of position and velocity errors, of the $i$th-manipulator within a multiple robot network, are proposed. The controllers employ adaptive techniques to find an estimate of the physical parameters of the nonlinear dynamics of the robot network. Moreover, the controllers can deal with different connectivity topologies (ring and star) and and can handle time-delays in the communications. Simulations, using a ten robot manipulators network with different connectivity topologies, that confirm the theoretical results are presented.**

## I. Introduction

One of the basic applications that require synchronization of multiple manipulators is teleoperators control [1], [2], [3]. In this paper we extend our previous results on control of bilateral teleoperators [4] to the more general problem of nonlinear synchronization of multiple robot manipulators with coupling time-delays.

Motivated by applications in physics, biology and engineering the study of synchronization of collections of dynamic systems has become an important topic in control theory [5], [6], [7]. Particularly, Cheong et al. [8] achieve state synchronization on a ring topology of interconnected linear dynamical systems using Smith predictors. Yao et al. [9] address the problem of synchronizing complex dynamical networks employing passivity-based control and linearization. Passivity is also exploited by Chopra and Spong [10] to demonstrate finite $\mathcal{L}_2$-gain of interconnected systems with time-delays. Rodriguez and Nijmeijer [11], using an exact model controller together with nonlinear observers, achieve position synchronization of cooperative manipulators. Adaptive control has been employed in several works. Among them, Sun and Mills [12] propose a controller capable of coordinating multirobot systems without time-delays using an integral term of the synchronization error. Applying contraction analysis [13], Chung and Slotine [14] present a general framework for the synchronization of Lagrangian systems with different network topologies. Zhu [15] analyzes the internal forces of manipulated objects and includes rigid constraints in the controller synthesis.

This paper employs adaptive control to deal with two basic problems: 1) synchronization of positions and velocities of a network of $m-$robots; 2) position and velocity tracking of a given desired trajectory. First the position error with regards to a given network topology, namely ring or star, and with a given connectivity, namely unilateral or bilateral, is defined. Then two controllers capable of solving the aforementioned problems are presented. The main novelty of this approach, which distinguishes it from existing techniques, is the use of *nonlinear couplings* among the agents in the proposed control law. Although nonlinear couplings have already been studied in [5], [16], they have been restricted to be first–third quadrant, to preserve the passivity properties required for the stability analysis. It should be underscored that the second controller does not need acceleration measurements in order to prove asymptotic synchronization of positions and velocities. Finally, some simulations with ten 2-Degrees Of Freedom (DOF) manipulators with different physical parameters are performed.

[1] Computer Science Department. University of Guadalajara (UDG). Guadalajara, Mexico.

[2] Institute of Industrial and Control Engineering (IOC). Technical University of Catalonia (UPC). Barcelona, Spain.

[3] Laboratoire des Signaux et Systèmes. SUPÉLEC. Gif-sur-Yvette, France.

*E-mail: emmanuel.nuno@upc.edu, luis.basanez@upc.edu, ortega@lss.supelec.fr*

## II. $m-$Robots Network Dynamics

The dynamic behavior of a $n$-DOF manipulator can be derived from the Euler-Lagrange equations of motion

$$L(\mathbf{q},\dot{\mathbf{q}}) = \frac{1}{2}\dot{\mathbf{q}}^\top \mathbf{M}(\mathbf{q})\dot{\mathbf{q}} - U(\mathbf{q}); \quad \frac{d}{dt}\frac{\partial L}{\partial \dot{\mathbf{q}}} - \frac{\partial L}{\partial \mathbf{q}} = \boldsymbol{\tau}$$

where $L(\mathbf{q},\dot{\mathbf{q}})$ is the so-called Lagrangian and $U(\mathbf{q})$ is the potential energy. $\dot{\mathbf{q}}, \mathbf{q} \in \mathbb{R}^n$ are the joint velocity and position and $\mathbf{M}(\mathbf{q}) \in \mathbb{R}^{n\times n}$ is the inertia matrix. These equations can be written as $\mathbf{M}(\mathbf{q})\ddot{\mathbf{q}} + \mathbf{C}(\mathbf{q},\dot{\mathbf{q}})\dot{\mathbf{q}} + \mathbf{g}(\mathbf{q}) = \boldsymbol{\tau}$, where $\ddot{\mathbf{q}} \in \mathbb{R}^n$ is the joint acceleration; $\mathbf{C}(\mathbf{q},\dot{\mathbf{q}}) \in \mathbb{R}^{n\times n}$ is the Coriolis and centrifugal effect; $\mathbf{g}(\mathbf{q}) = \frac{\partial U(\mathbf{q})}{\partial \mathbf{q}} \in \mathbb{R}^n$ is the gravitational force and $\boldsymbol{\tau} \in \mathbb{R}^n$ is a generalized force. This manipulator dynamics posses some important and well–known properties [17], [18]:

P1. $0 < \lambda_m\{\mathbf{M}(\mathbf{q})\}\mathbf{I} \leq \mathbf{M}(\mathbf{q}) \leq \lambda_M\{\mathbf{M}(\mathbf{q})\}\mathbf{I} < \infty$
P2. $\dot{\mathbf{M}}(\mathbf{q}) = \mathbf{C}(\mathbf{q},\dot{\mathbf{q}}) + \mathbf{C}^\top(\mathbf{q},\dot{\mathbf{q}})$
P3. $\exists k_c \in \mathbb{R}_{>0} : \ |\mathbf{C}(\mathbf{q},\dot{\mathbf{q}})\dot{\mathbf{q}}| \leq k_c|\dot{\mathbf{q}}|^2$.
P4. $\mathbf{M}(\mathbf{q})\ddot{\mathbf{q}} + \mathbf{C}(\mathbf{q},\dot{\mathbf{q}})\dot{\mathbf{q}} + \mathbf{g}(\mathbf{q}) = \mathbf{Y}(\mathbf{q},\dot{\mathbf{q}},\ddot{\mathbf{q}})\boldsymbol{\theta}$

where, in P4, $\mathbf{Y}(\mathbf{q},\dot{\mathbf{q}},\ddot{\mathbf{q}}) \in \mathbb{R}^{n\times p}$ is a regressor matrix of known functions and $\boldsymbol{\theta} \in \mathbb{R}^p$ is a constant vector with the manipulator physical parameters (link masses, moments of inertia, etc.).

The dynamics of a network of $m-$robots with different values of physical parameters, i.e., different inertia and Coriolis matrices, and different gravity vectors, are

$$\mathbf{M}_i(\mathbf{q}_i)\ddot{\mathbf{q}}_i + \mathbf{C}_i(\mathbf{q}_i,\dot{\mathbf{q}}_i)\dot{\mathbf{q}}_i + \mathbf{g}_i(\mathbf{q}_i) = \boldsymbol{\tau}_i \qquad (1)$$

where $i \in \bar{m} := \{1,...,m\}$. It is assumed that the manipulators consist of fully actuated revolute joints.

## III. NETWORK TOPOLOGY

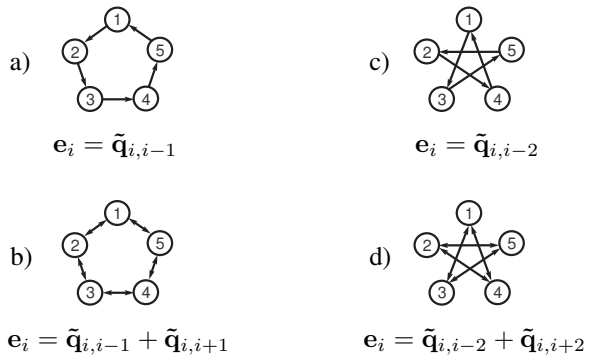


Fig. 1. Network topologies for a group of 5 robot manipulators and their corresponding position error function. a) unilateral ring, b) bilateral ring, c) unilateral star, d) bilateral star.

Each manipulator can be seen as a node of a network (graph) and its interconnection with other manipulators (nodes) can be defined using different network topologies. If the robot manipulators are connected, for example, using an unilateral ring topology, then the position error of the $i$th-manipulator can be defined as $\mathbf{e}_i = \mathbf{q}_i - \mathbf{q}_{i-1}(t - T_{i,i-1})$, where $T_{i,i-1}$ is the coupling time-delay from robot $i-1$ to $i$. If the interconnection is bilateral then $\mathbf{e}_i = 2\mathbf{q}_i - \mathbf{q}_{i-1}(t - T_{i,i-1}) - \mathbf{q}_{i+1}(t - T_{i,i+1})$. It should be noted that all indexes are modulus $m$ and are contained in the set $\bar{m}$, e.g., $\mathbf{q}_0 = \mathbf{q}_m$, $\mathbf{q}_{-1} = \mathbf{q}_{m-1}$, $\mathbf{q}_{m+1} = \mathbf{q}_1$ and $\mathbf{q}_{m+2} = \mathbf{q}_2$.

From graph theory, in the absence of time-delays, these error functions can be generalized using a Laplacian matrix $\mathbf{L} \in \mathbb{R}^{m \times m}$, relating the $i$th- and the $j$th-robot manipulators, as

$$\mathbf{e} = (\mathbf{L} \otimes \mathbf{I})\text{col}(\mathbf{q}_1, \mathbf{q}_2, ..., \mathbf{q}_m)$$

where $\mathbf{e} = \text{col}(\mathbf{e}_1, ..., \mathbf{e}_m)$, $\mathbf{I}$ is a $n \times n$ identity matrix and $\otimes$ is the Kronecker product [19], [20]. The topologies presented in this paper correspond to balanced and strongly connected graphs. For which, $|\mathbf{e}| \to 0 \Leftrightarrow \mathbf{q} \to (\alpha \mathbf{1}_m \otimes \mathbf{q}_0)$, $\forall \alpha \in \mathbb{R}, \mathbf{q_0} \in \mathbb{R}^n$ and $\mathbf{1}_m = \text{col}(1, \ldots, 1)$.

In order to analyze time-delays in the interconnections, let us start by defining the variable $\tilde{\mathbf{q}}_{i,j} \in \mathbb{R}^n$, that relates the position of the $i$th- and the $j$th-robot manipulators, as

$$\tilde{\mathbf{q}}_{i,j} = \mathbf{q}_i - \mathbf{q}_j(t - T_{i,j}).$$

The position error, of the different robot network topologies covered in this paper (see Fig.1), is given by

$$\begin{aligned} \mathbf{e}_i &= \tilde{\mathbf{q}}_{i,i-k} + (c-1)\tilde{\mathbf{q}}_{i,i+k} \\ &= c\mathbf{q}_i - \mathbf{q}_{i-k}(t - T_{i,i-k}) - (c-1)\mathbf{q}_{i+k}(t - T_{i,i+k}) \end{aligned}$$

where $c \in \{1, 2\}$ is the connectivity degree. $c = 1$ stands for unilateral connectivity and $c = 2$ for bilateral connectivity. $k \in \{1, 2\}$ is the adjacency index. $k = 1$ represents a ring topology and $k = 2$ a star topology. The corresponding velocity error is

$$\begin{aligned} \dot{\mathbf{e}}_i &= \dot{\tilde{\mathbf{q}}}_{i,i-k} + (c-1)\dot{\tilde{\mathbf{q}}}_{i,i+k} \\ &= c\dot{\mathbf{q}}_i - \dot{\mathbf{q}}_{i-k}(t - T_{i,i-k}) - (c-1)\dot{\mathbf{q}}_{i+k}(t - T_{i,i+k}). \end{aligned} \quad (2)$$

For the unilateral topologies ($c = 1$), such as Fig.1.a and Fig.1.c, $\mathbf{e}_i = \tilde{\mathbf{q}}_{i,i-k}$. On the other hand, for bilateral topologies ($c = 2$), such as Fig.1.b and Fig.1.d, $\mathbf{e}_i = \tilde{\mathbf{q}}_{i,i-k} + \tilde{\mathbf{q}}_{i,i+k}$. Consequently, $\dot{\mathbf{e}}_i = \dot{\tilde{\mathbf{q}}}_{i,i-k}$ and $\dot{\mathbf{e}}_i = \dot{\tilde{\mathbf{q}}}_{i,i-k} + \dot{\tilde{\mathbf{q}}}_{i,i+k}$, respectively.

*Remark 1:* In this paper we assume that $m \geq k + 1$. On the other hand, the network topologies covered in the paper are strongly connected and balanced, which means that, there exists a directed path from robot $i$ to robot $j$ and a directed path from $j$ to $i$ for every pair $i, j \in \bar{m}$, and every robot exchanges information with the same number of robots. These facts allow to show that synchronization is achieved when $|\mathbf{e}_i| \to 0$, in this scenario,

$$\mathbf{q}_i \to \frac{1}{c}[\mathbf{q}_{i-k}(t - T_{i,i-k}) + (c-1)\mathbf{q}_{i+k}(t - T_{i,i+k})],$$

and the only solution is all $\mathbf{q}_i$ be the same, e.g., for $c = 1, k = 1$, $\mathbf{q}_i \to \mathbf{q}_{i-1}(t - T_{i,i-1})$, and for illustration purposes consider $T_{i,j} = 0$, thus $\mathbf{q}_1 \to \mathbf{q}_m$, $\mathbf{q}_2 \to \mathbf{q}_1$ ... $\mathbf{q}_m \to \mathbf{q}_{m-1}$. Hence, $\mathbf{q}_1 \to \mathbf{q}_m \to \mathbf{q}_{m-1} \to ... \to \mathbf{q}_1$.

## IV. ACCELERATION BASED CONTROLLERS

In this section two controllers are presented. In the first of them, it is considered that the nonlinear model is known, and in the second, adaptive control is employed to provide asymptotic stability.

### A. The Known Model Approach

Let us define a *synchronizing signal* as

$$\mathbf{r}_i = \dot{\mathbf{e}}_i + \boldsymbol{\lambda}\mathbf{e}_i, \quad (3)$$

where $\boldsymbol{\lambda}$ is a diagonal positive definite matrix.

The proposed controllers are

$$\begin{aligned} \boldsymbol{\tau}_i = \tfrac{1}{c}\,(&\mathbf{M}_i\,[\ddot{\mathbf{q}}_{i-k}(t - T_{i,i-k}) + (c-1)\ddot{\mathbf{q}}_{i+k}(t - T_{i,i+k}) - \boldsymbol{\lambda}\dot{\mathbf{e}}_i] + \\ &+\mathbf{C}_i\,[\dot{\mathbf{q}}_{i-k}(t - T_{i,i-k}) + (c-1)\dot{\mathbf{q}}_{i+k}(t - T_{i,i+k}) - \boldsymbol{\lambda}\mathbf{e}_i] + \\ &+ \mathbf{g}_i - \mathbf{K}_i\mathbf{r}_i) \end{aligned} \quad (4)$$

where $\mathbf{K}_i = \mathbf{K}_i^\top > 0$. Substituting controllers (4) on the system dynamics (1), using (3), yields

$$\mathbf{M}_i(\mathbf{q}_i)\dot{\mathbf{r}}_i + \mathbf{C}_i(\mathbf{q}_i, \dot{\mathbf{q}}_i)\mathbf{r}_i + \mathbf{K}_i\mathbf{r}_i = \mathbf{0} \quad (5)$$

For any connectivity and any topology in Fig 1, with any coupling delays $T_{i,j}$, it is trivial to prove that, setting $\lambda_m\{\mathbf{K}_i\} > \lambda_M\{\mathbf{M}_i\}$, $|\mathbf{r}_i| \to 0$ exponentially. Take $V_i = \frac{1}{2}\mathbf{r}_i^\top \mathbf{M}_i(\mathbf{q}_i)\mathbf{r}_i$. Using (5) and P2, yields $\dot{V}_i \leq \lambda_m\{\mathbf{K}_i\}|\mathbf{r}_i|^2$. And invoking Lemma 1, which is presented in the Appendix, it is also proved that $|\dot{\mathbf{e}}_i| \to 0$ and $|\mathbf{e}_i| \to 0$.

### B. The Adaptive Control Approach

The adaptive version of (4) is

$$\begin{aligned} \boldsymbol{\tau}_i = \tfrac{1}{c}\,\Big(&\hat{\mathbf{M}}_i\,[\ddot{\mathbf{q}}_{i-k}(t - T_{i,i-k}) + (c-1)\ddot{\mathbf{q}}_{i+k}(t - T_{i,i+k}) - \boldsymbol{\lambda}\dot{\mathbf{e}}_i] + \\ &+\hat{\mathbf{C}}_i\,[\dot{\mathbf{q}}_{i-k}(t - T_{i,i-k}) + (c-1)\dot{\mathbf{q}}_{i+k}(t - T_{i,i+k}) - \boldsymbol{\lambda}\mathbf{e}_i] + \\ &+ \hat{\mathbf{g}}_i - \mathbf{K}_i\mathbf{r}_i) \end{aligned} \quad (6)$$

where $\hat{\mathbf{M}}_i, \hat{\mathbf{C}}_i, \hat{\mathbf{g}}_i$ are the estimates of the inertia and Coriolis matrices, and the gravity forces, respectively.

From P4, these controllers can be also written as

$$\boldsymbol{\tau}_i = \mathbf{Y}_i(\mathbf{q}_i, \dot{\mathbf{q}}_i, \mathbf{e}_i, \dot{\mathbf{e}}_i, \dot{\mathbf{q}}_{i-k}, \ddot{\mathbf{q}}_{i+k})\hat{\boldsymbol{\theta}}_i - \mathbf{K}_i\mathbf{r}_i$$

where $\mathbf{Y}_i$ are the regressor matrices of known functions, $\hat{\boldsymbol{\theta}}_i$ are the physical estimated parameters.

Similar to (5), substituting (6) on (1), yields

$$\mathbf{M}_i(\mathbf{q}_i)\dot{\mathbf{r}}_i + \mathbf{C}_i(\mathbf{q}_i, \dot{\mathbf{q}}_i)\mathbf{r}_i + \mathbf{K}_i\mathbf{r}_i = \mathbf{Y}_i\tilde{\boldsymbol{\theta}}_i = \boldsymbol{\Psi}_i \quad (7)$$

where $\tilde{\boldsymbol{\theta}}_i = \hat{\boldsymbol{\theta}}_i - \boldsymbol{\theta}_i$ are the errors between the estimation and the unknown real parameters.

*Remark 2:* As first shown in [21], (7) defines an output strictly passive map $\boldsymbol{\Psi}_i \mapsto \mathbf{r}_i$. Consider $V_i = \frac{1}{2}\mathbf{r}_i^\top\mathbf{M}_i(\mathbf{q}_i)\mathbf{r}_i$ as a storage function. From which, after evaluating along (7), it can be obtained $\dot{V}_i \leq \mathbf{r}_i^\top\boldsymbol{\Psi}_i - \lambda_m\{\mathbf{K}_i\}|\mathbf{r}_i|^2$. Integrating from 0 to $t$, and due to $V_i > 0$, yields $\int_0^t \mathbf{r}_i^\top\boldsymbol{\Psi}_i d\sigma \geq \lambda_m\{\mathbf{K}_i\}\|\mathbf{r}_i\|_2^2 - V_i(0)$. This suggests that if it is possible to generate a passive map $-\mathbf{r}_i \mapsto \boldsymbol{\Psi}_i$ then $\mathbf{r}_i \in \mathcal{L}_2$. This is due to the well-known passivity theorem that ensures $\mathcal{L}_2$-stability of the feedback interconnection of a passive and an output strictly passive map [22].

*Remark 3:* It is easy to prove that the map $-\mathbf{r}_i \mapsto \boldsymbol{\Psi}_i$ is passive with the following parameter estimation law

$$\dot{\hat{\boldsymbol{\theta}}}_i = -\boldsymbol{\Gamma}_i\mathbf{Y}_i^\top\mathbf{r}_i, \quad (8)$$

where $\boldsymbol{\Gamma}_i = \boldsymbol{\Gamma}_i^\top > 0$ and $\mathbf{Y}_i$ is defined as in (6). Note that, due to $\dot{\tilde{\boldsymbol{\theta}}}_i = \dot{\hat{\boldsymbol{\theta}}}_i$, $\mathbf{r}_i^\top\boldsymbol{\Psi}_i = \mathbf{r}_i^\top\mathbf{Y}_i\tilde{\boldsymbol{\theta}}_i = -\tilde{\boldsymbol{\theta}}_i^\top\boldsymbol{\Gamma}_i^{-1}\dot{\tilde{\boldsymbol{\theta}}}_i$. Hence, $-\int_0^t \mathbf{r}_i^\top\boldsymbol{\Psi}_i d\sigma = \int_0^t \tilde{\boldsymbol{\theta}}_i^\top\boldsymbol{\Gamma}_i^{-1}\dot{\tilde{\boldsymbol{\theta}}}_i d\sigma = \frac{1}{2}\tilde{\boldsymbol{\theta}}_i^\top\boldsymbol{\Gamma}_i^{-1}\tilde{\boldsymbol{\theta}}_i - \kappa_i \geq -\kappa_i$, where $\kappa_i = \frac{1}{2}\tilde{\boldsymbol{\theta}}_i^\top(0)\boldsymbol{\Gamma}_i^{-1}\tilde{\boldsymbol{\theta}}_i(0)$. Thus $-\mathbf{r}_i \mapsto \boldsymbol{\Psi}_i$ is passive.

*Proposition 1:* Consider (7) with the estimation law (8). Then, for any robot network topology and independently of the magnitude of the constant coupling time-delays $T_{i,j}$, $|\mathbf{e}_i|, |\dot{\mathbf{e}}_i|, |\mathbf{r}_i| \to 0$ as $t \to \infty$.

*Proof:* Consider $V_i = \frac{1}{2}\mathbf{r}_i^\top\mathbf{M}_i(\mathbf{q}_i)\mathbf{r}_i + \frac{1}{2}\tilde{\boldsymbol{\theta}}_i^\top\boldsymbol{\Gamma}_i^{-1}\tilde{\boldsymbol{\theta}}_i$, $V_i$ is positive definite and radially unbounded w.r.t $\mathbf{r}_i$ and $\tilde{\boldsymbol{\theta}}_i$. Evaluating $\dot{V}$ on (7) and (8), yields $\dot{V} = -\mathbf{r}_i^\top\mathbf{K}_i\mathbf{r}_i$. Hence, $\mathbf{r}_i \in \mathcal{L}_2 \cap \mathcal{L}_\infty$ and $\tilde{\boldsymbol{\theta}}_i \in \mathcal{L}_\infty$. From (3), $\mathbf{E}_i(s) = (s\mathbf{I} + \boldsymbol{\lambda})^{-1}\mathbf{R}_i(s)$, where $s$ is the Laplace variable, hence from Lemma 1, it follows that $\mathbf{e}_i \in \mathcal{L}_2 \cap \mathcal{L}_\infty$, $\dot{\mathbf{e}}_i \in \mathcal{L}_2$, and $|\mathbf{e}_i| \to 0$ as $t \to \infty$. Boundedness of $\mathbf{Y}_i$ is established with $\mathbf{r}_i, \tilde{\boldsymbol{\theta}}_i \in \mathcal{L}_\infty$. Hence, from (7) and P1, it can be concluded that $\dot{\mathbf{r}}_i \in \mathcal{L}_\infty$ and, by Barbălat's Lemma, $|\mathbf{r}_i| \to 0$, consequently $|\dot{\mathbf{e}}_i| \to 0$. ■

## V. Velocity Based Controllers

### A. The Known Model Approach

In this case the *synchronizing signal* is given by

$$\boldsymbol{\epsilon}_i = \dot{\mathbf{q}}_i + \boldsymbol{\lambda}\mathbf{e}_i. \quad (9)$$

An interesting fact of strongly connected and balanced graphs, that will be used in the proofs, is that $\sum_{i=1}^N\sum_{k=1}^n \epsilon_{i_k} = \sum_{i=1}^N\sum_{k=1}^n \dot{q}_{i_k}$, when $T_{i,j} = 0$. This follows from the fact that the Laplacian $\mathbf{L} \in \mathbb{R}^{m\times m}$ of such graph has a left eigenvector of all ones [19]. Thus, if we define $\mathbf{e} \in \mathbb{R}^{mn}$ –similarly to $\mathbf{q}$—piling up the $m$ components $\mathbf{e}_i$ we can write (9) as $\boldsymbol{\epsilon} = \dot{\mathbf{q}} + (\mathbf{L} \otimes \boldsymbol{\Lambda})\mathbf{q}$.

The proposed velocity-based controllers, for the $i$th-manipulator, are

$$\boldsymbol{\tau}_i = -\mathbf{M}_i(\mathbf{q}_i)\boldsymbol{\lambda}\dot{\mathbf{e}}_i - \mathbf{C}_i(\mathbf{q}_i, \dot{\mathbf{q}}_i)\boldsymbol{\lambda}\mathbf{e}_i + \mathbf{g}_i - \mathbf{K}_i\boldsymbol{\epsilon}_i - \mathbf{B}\dot{\mathbf{e}}_i. \quad (10)$$

where $\mathbf{K}_i = \mathbf{K}_i^\top > 0$ and $\mathbf{B} > 0$ is diagonal. Using (9) and (10) we can write (1) as

$$\mathbf{M}_i(\mathbf{q}_i)\dot{\boldsymbol{\epsilon}}_i + \mathbf{C}_i(\mathbf{q}_i, \dot{\mathbf{q}}_i)\boldsymbol{\epsilon}_i + \mathbf{K}_i\boldsymbol{\epsilon}_i + \mathbf{B}\dot{\mathbf{e}}_i = \mathbf{0}. \quad (11)$$

*Remark 4:* If we remove $\mathbf{B}\dot{\mathbf{e}}_i$ from (10), yields $\mathbf{M}_i(\mathbf{q}_i)\dot{\boldsymbol{\epsilon}}_i + \mathbf{C}_i(\mathbf{q}_i, \dot{\mathbf{q}}_i)\boldsymbol{\epsilon}_i + \mathbf{K}_i\boldsymbol{\epsilon}_i = \mathbf{0}$, which is similar to (5). Exponential convergence of $\boldsymbol{\epsilon}_i$ to zero can be easily proved with $V_i = \frac{1}{2}\boldsymbol{\epsilon}_i^\top\mathbf{M}_i(\mathbf{q}_i)\boldsymbol{\epsilon}_i$. However, due to the form of (9), Lemma 1 cannot ensure convergence of $\mathbf{e}_i$ to zero. This is precisely the reason why $\mathbf{B}\dot{\mathbf{e}}_i$ has to be included in the controllers.

*Proposition 2:* Consider (11). Then, for any robot network topology and for any constant coupling time-delays $T_{i,j}$, position errors and velocities asymptotically converge to zero.

*Proof:* Consider the following Lyapunov-Krasovskiĭ functional

$$V = \frac{1}{2}\sum_{i=1}^m \left[\boldsymbol{\epsilon}_i^\top\mathbf{M}_i\boldsymbol{\epsilon}_i + \mathbf{e}_i^\top\boldsymbol{\lambda}\mathbf{B}\mathbf{e}_i + c\int_{t-T_{i,j}}^{t} \dot{\mathbf{q}}_i^\top\mathbf{B}\dot{\mathbf{q}}_i d\sigma\right] \quad (12)$$

where $c \in \{1, 2\}$ represents the connectivity order. $V$ is positive definite and radially unbounded in $\boldsymbol{\epsilon}_i, \mathbf{e}_i$. Its time-derivative along (11), using P2, is given by

$$\begin{aligned}\dot{V} = &- \sum_{i=1}^m \left[\boldsymbol{\epsilon}_i^\top\mathbf{K}_i\boldsymbol{\epsilon}_i + \dot{\mathbf{q}}_i^\top\mathbf{B}\dot{\mathbf{e}}_i\right] + \\ &+ \sum_{i=1}^m \left[\frac{c}{2}(\dot{\mathbf{q}}_i^\top\mathbf{B}\dot{\mathbf{q}}_i - \dot{\mathbf{q}}_i^\top(t - T_{i,j})\mathbf{B}\dot{\mathbf{q}}_i(t - T_{i,j}))\right].\end{aligned} \quad (13)$$

Factoring $\mathbf{B}$ and invoking Lemma 2 to the resulting term, yields, for $c = 1$, $\dot{V} = -\sum_{i=1}^m \left[\boldsymbol{\epsilon}_i^\top\mathbf{K}_i\boldsymbol{\epsilon}_i + \frac{1}{2}\dot{\tilde{\mathbf{q}}}_{i,i-k}^\top\mathbf{B}\dot{\tilde{\mathbf{q}}}_{i,i-k}\right]$, and for $c = 2$,

$$\dot{V} = -\sum_{i=1}^m \left[\boldsymbol{\epsilon}_i^\top\mathbf{K}_i\boldsymbol{\epsilon}_i + \frac{1}{2}(\dot{\tilde{\mathbf{q}}}_{i,i-k}^\top\mathbf{B}\dot{\tilde{\mathbf{q}}}_{i,i-k} + \dot{\tilde{\mathbf{q}}}_{i,i+k}^\top\mathbf{B}\dot{\tilde{\mathbf{q}}}_{i,i+k})\right].$$

In both cases, $V \geq 0$ and $\dot{V} \leq 0$. Hence, $\boldsymbol{\epsilon}_i \in \mathcal{L}_2$ and $\boldsymbol{\epsilon}_i, \mathbf{e}_i \in \mathcal{L}_\infty$. Note that, for $c = 1$, $\dot{\tilde{\mathbf{q}}}_{i,i-k} \in \mathcal{L}_2$ and for $c = 2$, $\dot{\tilde{\mathbf{q}}}_{i,i-k}, \dot{\tilde{\mathbf{q}}}_{i,i+k} \in \mathcal{L}_2$, implying that $\dot{\mathbf{e}}_i \in \mathcal{L}_2$. From (9) one can also conclude that $\dot{\mathbf{q}}_i \in \mathcal{L}_\infty$, hence $\dot{\mathbf{e}}_i \in \mathcal{L}_\infty$.

From (15), it can be shown that $\dot{\boldsymbol{\epsilon}}_i \in \mathcal{L}_\infty$. Hence, with $\boldsymbol{\epsilon}_i \in \mathcal{L}_\infty \cap \mathcal{L}_2$, $\dot{\boldsymbol{\epsilon}}_i \in \mathcal{L}_\infty$ it is proved that $\boldsymbol{\epsilon}_i \to 0$.

$\dot{\boldsymbol{\epsilon}}_i, \dot{\mathbf{e}}_i \in \mathcal{L}_\infty$ imply that $\ddot{\mathbf{q}}_i \in \mathcal{L}_\infty$, hence $\ddot{\mathbf{e}}_i \in \mathcal{L}_\infty$. This last, and the fact that $\dot{\mathbf{e}}_i \in \mathcal{L}_\infty \cap \mathcal{L}_2$ prove that $|\dot{\mathbf{e}}_i| \to 0$.

Now, $\mathbf{e}_i, \dot{\mathbf{e}}_i, \ddot{\mathbf{e}}_i \in \mathcal{L}_\infty$ and $|\dot{\mathbf{e}}_i| \to 0$ imply that $\lim_{t\to\infty}\int_0^t \dot{\mathbf{e}}_i d\sigma = \mathbf{e}_i - \mathbf{e}_i(0) = k_i < \infty$. On the other hand,

$$\lim_{t\to\infty}|\boldsymbol{\epsilon}_i| = \lim_{t\to\infty}|\dot{\mathbf{q}}_i + \boldsymbol{\lambda}\mathbf{e}_i| = \lim_{t\to\infty}|\dot{\mathbf{q}}_i + \boldsymbol{\lambda}(k_i - \mathbf{e}_i(0))| = 0$$

imply that when $t \to \infty$, $\dot{\mathbf{q}}_i \to -\boldsymbol{\lambda}(k_i - \mathbf{e}_i(0))$ that is constant. This and $|\dot{\mathbf{e}}_i| \to 0$ ensure that $\mathbf{q}_i - \mathbf{q}_j(t - T_{i,j}) \to \mathbf{q}_i - \mathbf{q}_j$. Thus, in the limit we can use the Laplacian

matrix and its properties to show that $\sum_{i=1}^{N}\sum_{k=1}^{n}\epsilon_{i_k} = \sum_{i=1}^{N}\sum_{k=1}^{n}\dot{q}_{i_k}$. Hence, the fact that $|\boldsymbol{\epsilon}_i| \to 0$ implies that $\dot{\mathbf{q}}_i = \mathbf{0}$. Thus, $|\dot{\mathbf{q}}_i| \to |\mathbf{e}_i| \to 0$. This completes the proof. ■

### B. The Adaptive Control Approach

The proposed adaptive controllers are

$$\boldsymbol{\tau}_i = -\hat{\mathbf{M}}_i(\mathbf{q}_i)\boldsymbol{\lambda}\dot{\mathbf{e}}_i - \hat{\mathbf{C}}_i(\mathbf{q}_i,\dot{\mathbf{q}}_i)\boldsymbol{\lambda}\mathbf{e}_i + \hat{\mathbf{g}}_i - \mathbf{K}_i\boldsymbol{\epsilon}_i - \mathbf{B}\dot{\mathbf{e}}_i, \quad (14)$$

thus, $\boldsymbol{\tau}_i = \mathbf{Y}_i(\mathbf{q}_i,\dot{\mathbf{q}}_i,\mathbf{e}_i,\dot{\mathbf{e}}_i)\hat{\boldsymbol{\theta}}_i - \mathbf{K}_i\boldsymbol{\epsilon}_i - \mathbf{B}\dot{\mathbf{e}}_i$.

Using (9) and (14), (1) becomes

$$\mathbf{M}_i(\mathbf{q}_i)\dot{\boldsymbol{\epsilon}}_i + \mathbf{C}_i(\mathbf{q}_i,\dot{\mathbf{q}}_i)\boldsymbol{\epsilon}_i + \mathbf{K}_i\boldsymbol{\epsilon}_i + \mathbf{B}\dot{\mathbf{e}}_i = \mathbf{Y}_i\tilde{\boldsymbol{\theta}}_i = \boldsymbol{\Phi}_i \quad (15)$$

*Proposition 3:* Consider (15) together with the estimation law

$$\dot{\hat{\boldsymbol{\theta}}}_i = -\boldsymbol{\Gamma}_i\mathbf{Y}_i^{\top}\boldsymbol{\epsilon}_i. \quad (16)$$

Then, for any robot network topology and for any constant coupling time-delays $T_{i,j}$, the following holds $|\boldsymbol{\epsilon}_i| \to 0$ as $t \to \infty$. Moreover, $|\dot{\mathbf{q}}_i|, |\mathbf{e}_i| \to 0$.

*Proof:* The proof is established with function (12) plus the term $\frac{1}{2}\sum_{i=1}^{m}\tilde{\boldsymbol{\theta}}_i^{\top}\boldsymbol{\Gamma}_i^{-1}\tilde{\boldsymbol{\theta}}_i$. In this case such $V$ is positive definite and radially unbounded in $\boldsymbol{\epsilon}_i, \mathbf{e}_i, \tilde{\boldsymbol{\theta}}_i$, and its time-derivative along (15) and (16), using P2, is equal to (13). Hence $V \geq 0$ and $\dot{V} \leq 0$ for $c \in \{1,2\}$. Thus, $\boldsymbol{\epsilon}_i, \dot{\mathbf{e}}_i \in \mathcal{L}_2$ and $\boldsymbol{\epsilon}_i, \mathbf{e}_i, \tilde{\boldsymbol{\theta}}_i \in \mathcal{L}_\infty$. From (9) it is concluded that $\dot{\mathbf{q}}_i \in \mathcal{L}_\infty$, hence $\dot{\mathbf{e}}_i \in \mathcal{L}_\infty$. All these bounded signals imply that $\boldsymbol{\Phi}_i \in \mathcal{L}_\infty$.

The rest of the proof follows *verbatim* the proof of Proposition 2. ■

### C. Synchronization to a Common Desired Trajectory

Suppose now that the objective is to drive the manipulators to a common, twice differentiable, desired trajectory $\mathbf{q}_d \in \mathbb{R}^n$, in this scenario the position error of the $i$th-manipulator becomes

$$\mathbf{e}_i = (c{+}1)\mathbf{q}_i - \mathbf{q}_{i-k}(t - T_{i,i-k}) - (c-1)\mathbf{q}_{i+k}(t - T_{i,i+k}) - \mathbf{q}_d.$$

The acceleration based controllers (6), become

$$\begin{aligned}\boldsymbol{\tau}_i = \tfrac{1}{c+1}\big(&\hat{\mathbf{g}}_i - \mathbf{K}_i\mathbf{r}_i + \\ &+\hat{\mathbf{M}}_i\left[\ddot{\mathbf{q}}_{i-k}(t-T_{i,i-k}) + (c-1)\ddot{\mathbf{q}}_{i+k}(t-T_{i,i+k}) + \ddot{\mathbf{q}}_d - \boldsymbol{\lambda}\dot{\mathbf{e}}_i\right] + \\ &+\hat{\mathbf{C}}_i\left[\dot{\mathbf{q}}_{i-k}(t-T_{i,i-k}) + (c-1)\dot{\mathbf{q}}_{i+k}(t-T_{i,i+k}) + \dot{\mathbf{q}}_d - \boldsymbol{\lambda}\mathbf{e}_i\right]\big)\end{aligned}$$

from which we can recover (7) and Proposition 1 holds. Thus, in this scenario $|\mathbf{e}_i| \to 0$ for any $T_{i,j}$ and any connectivity topology.

The employment of $\mathbf{q}_d$ in controllers (14) leaves (15) unchanged. And, for a given constant $\mathbf{q}_d$, Proposition 3 holds.

## VI. Simulations

The simulations are performed with ten 2-DOF nonlinear manipulators with revolute joints. Their corresponding nonlinear dynamics are modeled by (1) where the elements of the inertia matrices $\mathbf{M}_i(\mathbf{q}_i)$ are $M_{i_{11}} = \alpha_i + 2\beta_i \mathrm{c}_{2_i}$, $M_{i_{12}} = M_{i_{21}} = \delta_i + \mathrm{c}_{2_i}$ and $M_{i_{22}} = \delta_i$; the elements of the Coriolis and centrifugal matrices $\mathbf{C}_i(\mathbf{q}_i,\dot{\mathbf{q}}_i)$ are $C_{i_{11}} = 2C_{i_{12}} = -2\beta_i \mathrm{s}_{2_i}\dot{q}_{2_i}$, $C_{i_{21}} = \beta_i \mathrm{s}_{2_i}\dot{q}_{1_i}$ and $C_{i_{21}} = 0$; and, finally, the elements of the gravity forces $\mathbf{g}_i(\mathbf{q}_i)$ are $g_{i_1} = \frac{1}{l_{2_i}}g\delta_i \mathrm{c}_{12_i} + \frac{1}{l_{1_i}}(\alpha_i - \delta_i)\mathrm{c}_{1_i}$ and $g_{i_2} = \frac{1}{l_{2_i}}g\delta_i \mathrm{c}_{12_i}$. In these expressions $\mathrm{c}_{2_i}$, $\mathrm{s}_{2_i}$ and $\mathrm{c}_{12_i}$ are the short notations for $\cos(q_{2_i})$, $\sin(q_{2_i})$ and $\cos(q_{1_i}+q_{2_i})$, respectively; $q_{z_i}$ is the articular position of link $z$ of manipulator $i$, with $z \in \{1,2\}$; $\dot{q}_{1_i}$ and $\dot{q}_{2_i}$ are the respective revolute velocities of the two links; $\alpha_i = l_{2_i}^2 m_{2_i} + l_{1_i}^2(m_{1_i} + m_{2_i})$, $\beta_i = l_{1_i} l_{2_i} m_{2_i}$ and $\delta_i = l_{2_i}^2 m_{2_i}$. $l_{k_i}$ and $m_{k_i}$ are the respective lengths and masses of each link.

The following parametrization is proposed for each manipulator

$$\mathbf{Y}(\mathbf{q},\dot{\mathbf{q}},\ddot{\mathbf{q}}) = \begin{bmatrix} \ddot{q}_1 & Y_{21} & \ddot{q}_2 & g\mathrm{c}_{12} & g\mathrm{c}_1 \\ 0 & \mathrm{c}_2\ddot{q}_1 + \mathrm{s}_2\dot{q}_1^2 & \ddot{q}_1 + \ddot{q}_2 & g\mathrm{c}_{12} & 0 \end{bmatrix},$$

$$\boldsymbol{\theta} = \begin{bmatrix} \alpha & \beta & \delta & \frac{1}{l_2}\delta & \frac{1}{l_1}(\alpha - \delta) \end{bmatrix}^{\top},$$

where $Y_{21} = 2\mathrm{c}_2\ddot{q}_1 + \mathrm{c}_2\ddot{q}_2 - \mathrm{s}_2\dot{q}_2^2 - 2\mathrm{s}_2\dot{q}_1\dot{q}_2$.

The physical parameters are: for manipulators $1, 2$ and $3$ the length of links $l_{1_{1,2,3}}$ and $l_{2_{1,2,3}}$ is $0.38$m, the masses at each link are $m_{1_{1,2,3}} = 3.9473$kg, $m_{2_{1,2,3}} = 0.6232$kg; for manipulators $4, 5$ and $6$ the length of links $l_{1_{4,5,6}}$ and $l_{2_{4,5,6}}$ is $0.48$m, the masses at each link are $m_{1_{4,5,6}} = 3.5473$kg, $m_{2_{4,5,6}} = 1.1232$kg; and for the last four, $7, 8, 9$ and $10$, $l_{1_{7,8,9,10}} = l_{2_{7,8,9,10}} = 0.55$m and $m_{1_{7,8,9,10}} = 2.9473$kg, $m_{2_{7,8,9,10}} = 0.8232$kg.

Due to space limitations, only simulations with the velocity based adaptive controller using a bilateral ring topology ($c = 2$ and $k = 1$) are presented. For this case $\boldsymbol{\lambda} = 2\mathbf{I}$ in (9), the matrices $\mathbf{Y}_i$ for (14) are given by

$$\begin{bmatrix} -\dot{e}_{l_i} & Y_{12} & -\dot{e}_{i_2} & g\mathrm{c}_{i_{12}} & g\mathrm{c}_{i_1} \\ 0 & -\mathrm{c}_{i_2}\dot{e}_{i_1} - \mathrm{s}_{i_2}\dot{q}_{i_1}e_{i_1} & -\dot{e}_{i_1} - \dot{e}_{i_2} & g\mathrm{c}_{i_{12}} & 0 \end{bmatrix}$$

where $Y_{12} = -2\mathrm{c}_{i_2}\dot{e}_{i_1} - \mathrm{c}_{i_2} - \dot{e}_{i_2} + \mathrm{s}_{i_2}\dot{q}_{i_2}e_{i_2} + 2\mathrm{s}_{i_2}\dot{q}_{i_2}e_{i_1}$.

The initial conditions are $\ddot{\mathbf{q}}_i(0) = \dot{\mathbf{q}}_i(0) = \mathbf{0}$ and all $\mathbf{q}_i(0)$ differ one from another. The controllers gains are: $\boldsymbol{\Gamma}_i = 4\mathbf{I}$, $\mathbf{K}_i = 15\mathbf{I}$ and $\mathbf{B} = 10\mathbf{I}$.

The first set of simulations depict the synchronization results from the different initial conditions without a common desired position. From Fig. 2 it can be observed that, when the coupling time-delays are negligible, i.e., $T_{i,j} = 0.01$s, the manipulators synchronize to the average of their initial conditions. Incrementing the coupling delays, such that $T_{i,j} = 0.5$s, results on more time to synchronize compared to negligible delays, as can be seen in Fig. 3. Moreover, when $t = T_{i,j} = 0.5$s it can be observed that the error grows due to the arrival of past data. Large time-delays induce an interesting behavior, as seen in Fig. 4 when $T_{i,j} = 3$s, that is the reproduction of the initial error every $t = nT_{i,j}$ for $n = 1, 2, ....$ In these three simulations, independently of the coupling time-delays, all manipulator position errors asymptotically converge to zero.

The second set of simulations deals with the synchronization to a common desired position $\mathbf{q}_d = [-1, 1]^{\top}$. Fig. 5 depicts a simulation for $T_{i,j} = 0.01$s, Fig. 6 for $T_{i,j} = 0.5$s and, finally, Fig. 7 for $T_{i,j} = 3$s. In all cases the manipulators positions synchronize at the desired position. Note, however, that as coupling time-delays increase, the

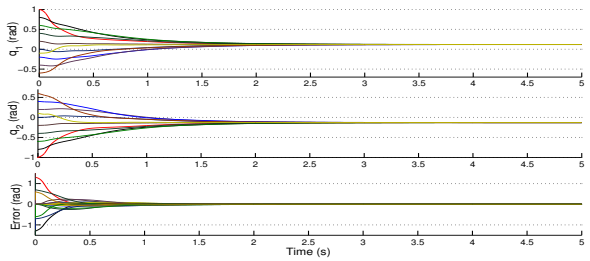


Fig. 2. Synchronization without a common trajectory with a bilateral ring topology and negligible time-delays, i.e., $T_{i,j} = 0.01$s.

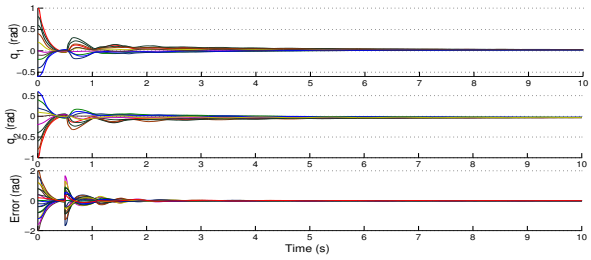


Fig. 3. Synchronization without a common trajectory with a bilateral ring topology where $T_{i,j} = 0.5$s.

manipulators require more time to reach the desired position, but they always move in a synchronous way.

## VII. Conclusions

This paper presents four controllers, two assuming the knowledge of the nonlinear model and two adaptive, able to synchronize the positions and velocities of a multiple robot network. It has been proved that synchronization occurs despite coupling time-delays. The robots of the network can track a common desired trajectory or, without such trajectory, can find a consensus. The main difference with prior works is that position error is used in the estimation law, and the position error of the $i$th-manipulator depends on the chosen connectivity topology, that can be either ring or star, unilateral or bilateral. Simulation results show the effectiveness of the proposed approaches. Future works will deal with variable coupling time-delays and more complex networks.

Recently, in [14], [23] an attempt has been made to extend the Slotine and Li controller to the case of networks of

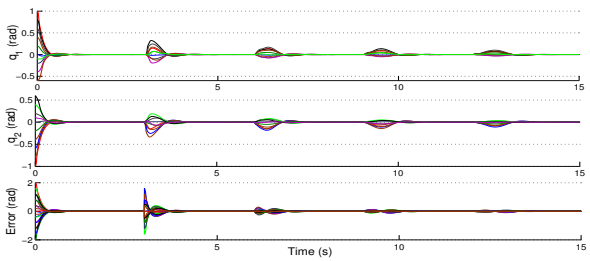


Fig. 4. Synchronization without a common trajectory with a bilateral ring topology and large coupling time-delays, i.e., $T_{i,j} = 3$s.

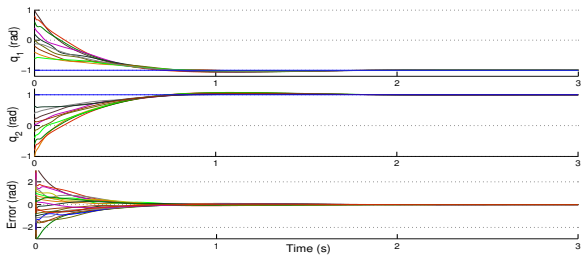


Fig. 5. Synchronization to a common desired position $\mathbf{q}_d = [-1, 1]^\top$rad using the acceleration-free controller with a bilateral ring topology and negligible time-delays, i.e., $T_{i,j} = 0.01$s.

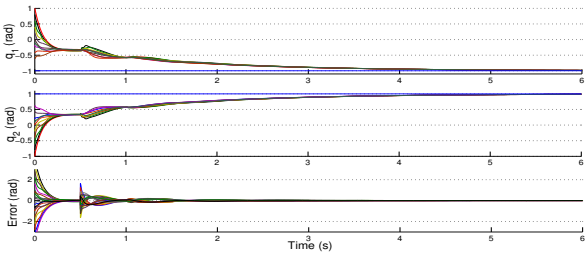


Fig. 6. Synchronization to a common desired position $\mathbf{q}_d = [-1, 1]^\top$rad using the acceleration-free controller with a bilateral ring topology and $T_{i,j} = 0.5$s.

EL systems. To put in perspective our contribution, we recall the closed–loop dynamics obtained in those papers, namely $\mathbf{M}_i\dot{\mathbf{s}}_i + \mathbf{C}_i\mathbf{s}_i + \mathbf{K}_1\mathbf{s}_i - \sum_j \mathbf{K}_2(\mathbf{s}_j - \mathbf{s}_i) = 0$ with $\mathbf{s}_i := \dot{\tilde{\mathbf{q}}}_i + \lambda\tilde{\mathbf{q}}_i$, the signal used in the classical Slotine and Li controller, and $\mathbf{K}_1, \mathbf{K}_2 \in \mathbb{R}^{n\times n}$ are some suitable gain matrices. A standard analysis with $\mathbf{s}^\top\mathbf{M}\mathbf{s}$ gives conditions on $\mathbf{K}_1, \mathbf{K}_2$ such that $\mathbf{s} \in \mathcal{L}_2$ and, consequently, that $\tilde{\mathbf{q}} \to 0$. This controller can track a desired trajectory but, in the absence of a reference position, drives all positions to zero.

Our current research proceeds along the following avenues.

- Generalizing the controllers for complex networks, modeled with balanced and connected graphs.
- Determining the convergence point of the positions, without adaptation, but in the face of communication delays.
- Studying the case of time varying communication de-

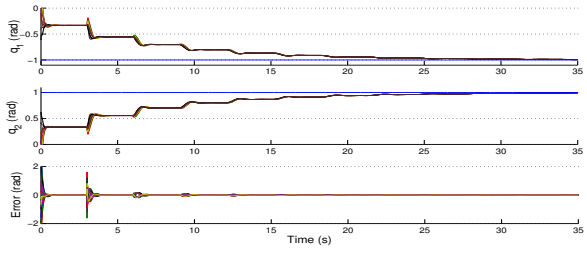


Fig. 7. Synchronization to a common desired position $\mathbf{q}_d = [-1, 1]^\top$rad using the acceleration-free controller with a bilateral ring topology and large coupling delays $T_{i,j} = 3$s.

lays. The results reported in [3] for teleoperators lead to believe that this is a feasible problem.

- Providing some design guidelines for the gains $\boldsymbol{\lambda}, \mathbf{B}_i, \mathbf{K}_i$ and $\boldsymbol{\Gamma}_i$. Although the stability results are valid for arbitrary positive values of these gains, simulations show that they play a key role on the transient performance, that should be clarified.

## APPENDIX

*Lemma 1:* Let $\mathbf{e}, \mathbf{r} \in \mathbb{R}^n$ and $\mathbf{E}(s) = \mathbf{H}(s)\mathbf{R}(s)$, where $\mathbf{H}(s)$ is an $n \times n$ strictly proper, exponentially stable transfer function and $s$ is the Laplace variable. Then $\mathbf{r} \in \mathcal{L}_2$ implies that $\mathbf{e} \in \mathcal{L}_2 \cap \mathcal{L}_\infty$, $\dot{\mathbf{e}} \in \mathcal{L}_2$, $\mathbf{e}$ is continuous, and $|\mathbf{e}| \to 0$ as $t \to \infty$. If, in addition, $|\mathbf{r}| \to 0$ as $t \to \infty$, $|\dot{\mathbf{e}}| \to 0$ [24].

*Lemma 2:* The following relation holds for $c \in \{1, 2\}$ and $k \in \{1, 2\}$.

$$\sum_{i=1}^{m} \left[ \frac{c}{2}(|\dot{\mathbf{q}}_i|^2 - |\dot{\mathbf{q}}_i(t - T_{i,j})|^2) - \dot{\mathbf{q}}_i^\top \dot{\mathbf{e}}_i \right] = \\ = -\frac{1}{2} \sum_{i=1}^{m} (|\dot{\tilde{\mathbf{q}}}_{i,i-k}|^2 + (c-1)|\dot{\tilde{\mathbf{q}}}_{i,i+k}|^2). \quad (17)$$

*Proof:* First note that the right hand side of (17), for $c = 1$ or $c = 2$, is $-\frac{1}{2}\sum_{i=1}^{m} |\dot{\tilde{\mathbf{q}}}_{i,i-k}|^2$ or $-\frac{1}{2}\sum_{i=1}^{m} (|\dot{\tilde{\mathbf{q}}}_{i,i-k}|^2 + |\dot{\tilde{\mathbf{q}}}_{i,i+k}|^2)$, respectively. The proof shows that the left hand side of (17) returns these same square terms for $c = 1$ or $c = 2$.

Let us substitute, on the left hand side of (17), the term $\dot{\mathbf{e}}_i$ in (2). This yields

$$\sum_{i=1}^{m} ( \quad - \quad \frac{c}{2}(|\dot{\mathbf{q}}_i|^2 + |\dot{\mathbf{q}}_i(t - T_{i,j})|^2) + \quad (18) \\ + \quad \dot{\mathbf{q}}_i^\top [\dot{\mathbf{q}}_{i-k}(t - T_{i,i-k}) + (c-1)\dot{\mathbf{q}}_{i+k}(t - T_{i,i+k})] )$$

Now, for $c = 1$, (18) becomes

$$\sum_{i=1}^{m} \left[ \dot{\mathbf{q}}_i^\top \dot{\mathbf{q}}_{i-k}(t - T_{i,i-k}) - \frac{1}{2}(|\dot{\mathbf{q}}_i|^2 + |\dot{\mathbf{q}}_i(t - T_{i,j})|^2) \right] \quad (19)$$

Now, the key part of the proof resides in the following relation $\sum_{i=1}^{m} |\dot{\mathbf{q}}_i(t - T_{i,j})|^2 = \sum_{i=1}^{m} |\dot{\mathbf{q}}_{i-k}(t - T_{i,i-k})|^2$, which is due to the fact that all indexes must be contained in the set $\bar{m}$, i.e., $i, i-k \in \bar{m}$, and as long as the sum covers all indexes, the relation holds. Hence, (19) changes to

$$\sum_{i=1}^{m} \left[ \dot{\mathbf{q}}_i^\top \dot{\mathbf{q}}_{i-k}(t - T_{i-k}) - \frac{1}{2}(|\dot{\mathbf{q}}_i|^2 + |\dot{\mathbf{q}}_{i-k}(t - T_{i,i-k})|^2) \right],$$

clearly, this is equal to $-\frac{1}{2}\sum_{i=1}^{m} |\dot{\tilde{\mathbf{q}}}_{i,i-k}|^2$.

Using the same procedure, with the additional fact that $\sum_{i=1}^{m} |\dot{\mathbf{q}}_i(t - T_{i,j})|^2 = \sum_{i=1}^{m} |\dot{\mathbf{q}}_{i+k}(t - T_{i,i+k})|^2$, it is concluded that, for $c = 2$, (18) is equal to $-\frac{1}{2}\sum_{i=1}^{m} (|\dot{\tilde{\mathbf{q}}}_{i,i-k}|^2 + |\dot{\tilde{\mathbf{q}}}_{i,i+k}|^2)$. ■

## ACKNOWLEDGEMENTS

This paper has been partially supported by the Spanish CICYT projects DPI2008-02448 and DPI2007-63665, FPI Ref. BES-2006-13393. The first author acknowledges the support of the CONACyT Mexico under the postdoctoral grant 121978.

## REFERENCES

[1] R.J. Anderson and M.W. Spong. Bilateral control of teleoperators with time delay. *IEEE Trans. on Automatic Control*, 34(5):494–501, May 1989.

[2] E. Nuño, R. Ortega, N. Barabanov, and L. Basañez. A globally stable PD controller for bilateral teleoperators. *IEEE Transactions on Robotics*, 24(3):753–758, June 2008.

[3] E. Nuño, L. Basañez, R. Ortega, and M.W. Spong. Position tracking for nonlinear teleoperators with variable time-delay. *The International Journal of Robotics Research*, 28(7):895–910, July 2009.

[4] E. Nuño, R. Ortega, and L. Basañez. An adaptive controller for nonlinear bilateral teleoperators. *Automatica*, 46(1):155–159, January 2010.

[5] R. Olfati-Saber, J.A. Fax, and R.M. Murray. Consensus and cooperation in networked multi-agent systems. *Proceeding of the IEEE*, 95(1):215–233, Jan. 2007.

[6] L. Scardovi and R. Sepulchre. Synchronization in networks of identical linear systems. *Automatica*, 45(11):2557–2562, Nov. 2009.

[7] L. Scardovi, M. Arcak, and E.D. Sontag. Synchronization of interconnected systems with applications to biochemical networks: An input-output approach. *IEEE Transactions on Automatic Control*, 55(6):1367–1379, June 2010.

[8] J. Cheong, S.I. Niculescu, and C. Kim. Motion synchronization control of distributed multisubsystems with invariant local natural dynamics. *IEEE Transactions on Robotics*, 25(2):582–598, April 2009.

[9] J. Yao, Z.H. Guan, and D.J. Hill. Passivity-based control and synchronization of general complex dynamical networks. *Automatica*, 45(9):2107–2113, Sept. 2009.

[10] N. Chopra and M.W. Spong. Delay independent stability for interconnected nonlinear systems with finite $\mathcal{L}_2$ gain. In *Proc. of the IEEE Conf. on Decision and Control*, pages 1–6, December 2007.

[11] A. Rodriguez-Angeles and H. Nijmeijer. Mutual synchronization of robots via estimated state feedback: A cooperative approach. *IEEE Transactions on Control Systems Technology*, 12(4):542–554, July 2004.

[12] D. Sun and J.K. Mills. Adaptive synchronized control for coordination of multirobot assembly tasks. *IEEE Transactions on Robotics and Automation*, 18(4):498–510, Aug. 2002.

[13] W. Wang and J.J. Slotine. Contraction analysis of time-delayed communications and group cooperation. *IEEE Trans. on Automatic Control*, 51(4):712–717, April 2006.

[14] S.J. Chung and J.J. Slotine. Cooperative robot control and concurrent synchronization of lagrangian systems. *IEEE Trans. on Robotics*, 25(3):686–700, June 2009.

[15] W.H. Zhu. On adaptive synchronization control of coordinated multirobots with flexible/rigid constraints. *IEEE Transactions on Robotics*, 21(3):520–525, June 2005.

[16] N. Chopra and M.W. Spong. Output synchronization of nonlinear systems with time delay in communication. In *Proc. of the IEEE Conf. on Decision and Control*, pages 4986–4992, December 2006.

[17] R. Kelly, V. Santibáñez, and A. Loria. *Control of robot manipulators in joint space*. Advanced textbooks in control and signal processing. Springer-Verlag, 2005.

[18] M.W. Spong, S. Hutchinson, and M. Vidyasagar. *Robot Modeling and Control*. Wiley, 2005.

[19] R. Olfati-Saber and R.M. Murray. Consensus problems in networks of agents with switching topology and time-delays. *IEEE Transactions on Automatic Control*, 49(9):1520–1533, Sept. 2004.

[20] M. Arcak. Passivity as a design tool for group coordination. *IEEE Transactions on Automatic Control*, 52(8):1380–1390, Aug. 2007.

[21] R. Kelly and R. Ortega. Adaptive control of robot manipulators: an input-output approach. In *Proc. of the IEEE Int. Conf. on Robotics and Automation*, volume 2, pages 699–703, April 1988.

[22] M. Vidyasagar. *Nonlinear Systems Analysis*. Prentice Hall, 1993.

[23] N. Chopra and Y.C. Liu. Controlled synchronization of mechanical systems. In *Proc. of 1st ASME Dynamic Systems and Control Conference*, Ann Arbor, Michigan, USA, Oct. 2008.

[24] R. Ortega and M. W. Spong. Adaptive motion control of rigid robots: a tutorial. *Automatica*, 25(6):877–888, 1989.